

Inertia emulation control technique based frequency control of grid-connected single-phase rooftop photovoltaic system with battery and supercapacitor

ISSN 1752-1416

Received on 24th July 2019

Revised 28th November 2019

Accepted on 19th December 2019

E-First on 16th April 2020

doi: 10.1049/iet-rpg.2019.0873

www.ietdl.org

Ratnam Kamala Sarojini¹, K. Palanisamy¹ ✉, P. Sanjeevikumar², Jens Bo-Holm Nielsen²

¹School of Electrical Engineering, Vellore Institute of Technology, Vellore, Tamil Nadu, India

²Department of Energy Technology, Center for Bioenergy and Green Engineering, Aalborg University, Esbjerg, Denmark

✉ E-mail: kpalanisamy@vit.ac.in

Abstract: With the increasing penetration of renewable energy sources in the power system, the power electronic inverters are widely used to interface with the grid, which will reduce the inertia of the power system. This study proposes ancillary inertial service from single-phase rooftop solar photovoltaic (PV) based inverter to the grid. The inertia emulation control technique transforms the behaviour of inverter like a synchronous generator under power imbalances. A hybrid energy storage system consisting of battery and supercapacitor (SC) has been connected at the DC bus to take care of the variability in PV output power and load fluctuations. The SC absorbs/injects the fast-varying power and provides the inertial response to arrest the frequency deviation and battery charges/discharges to bring back the frequency to the nominal value. Real-time simulation is carried out to test the system behaviour for different operating conditions using OPAL-RT 5700.

1 Introduction

The power generation from the renewable energy source (RES) is increasing continuously, to meet the raised electricity demand and with an increased emphasis on environmental rules. The environmentally friendly solar photovoltaic (PV) technology usage is developing in a faster way for grid-connected applications. Further, the RES advancement strategies around the world, like feed-in-tariff, net metering, etc. [1] are giving incentives to single-phase residential consumers also to install rooftop PV panels. The power loss can be reduced by generating the power near to the customers using rooftop PV panels. Hence, the installation of single-phase inverters is increasing in recent years to incorporate the rooftop PV panels with residential customers. If single-phase photovoltaic (SPV) inverters are properly controlled, then these can provide ancillary services to the grid. The single-phase rooftop PV inverters are generally intended to deal with the powers between 1 and 5 kW because of the area available for installation and investment. This paper presents a control algorithm for the SPV, to change the behaviour of inverter like synchronous generator under frequency variations.

The control of a grid-connected single-phase inverter with recurrent neural network-based vector control has been presented in [2] to decrease the harmonics. An adaptive harmonic compensation technique for the lower order harmonic compensation is presented in [3] for SPV. They demonstrate that the performance of the grid-connected single-phase inverter is enhanced with the reduced harmonic current. However, under the grid frequency deviation condition the performance is unknown. The single-phase inverter control using repetitive non-linear control for RES-based microgrid is proposed in [4]. The tailor-made current control solution is proposed in [5] can suppress the harmonics effectively than the repetitive control. However, these techniques do not participate in the frequency regulation.

The ripple power predictive control is proposed in [6] to compensate for the ripple power for single-phase grid-connected inverter. The active and reactive power control of three-phase grid-connected PV based inverter using dqo transformation is presented in [7, 8]. The vector control for the single-phase inverter using the orthogonal technique is presented in [9] to improve the performance. The vector control of grid-connected single-phase solar inverters proposed in [10], mainly aims to balance the DC bus

voltage and decoupling of active and reactive powers. To eliminate the adverse impact of proportional-integral (PI) control in vector control, the direct power control for the single-phase inverters is proposed in [11] using dead-beat strategy.

All the control techniques discussed in the literature for single-phase inverters are injecting constant power to the grid and do not react for the grid frequency variations. The frequency regulation capability is missing in the single-phase inverter control techniques. Not only in the single-phase grid-connected PV inverters but also the three-phase grid-connected PV inverters are operating at the maximum power point tracking (MPPT) technique to inject the maximum available power injecting into the grid as a current source irrespective of the grid frequency conditions, whereas grid-connected synchronous generator injects or absorbs the active power with respect to the frequency variations. Recently, some authors [12–15] proposed the control algorithms for the three-phase inverters to change the behaviour of the inverter like a synchronous generator. The controller has been designed in such a way that the inertial characteristics of the synchronous generator is emulated to regulate the frequency. Still, the research is going on for the frequency regulation capabilities for the three-phase grid-connected inverter. In [16], the researchers addressed the implementation of an inertia emulation control (IEC) for a single-phase inverter in the vehicle to grid application. For voltage and current control loops, the proportional resonant controller was used. However, the proportional resonant controller has to be tuned for a particular frequency and it does not work properly for frequencies other than tuned frequencies. In [16–19] the IEC is realised with an ideal voltage source connected to the inverter which is obviously not the real case. Energy storage systems should actually be included in IEC in order to achieve frequency control. Practically, the charging status of the battery must be considered in order to provide an inertial response to the grid. The single-phase synchronverter with hysteresis control is proposed in [20]. The switching frequency of the hysteresis controller varies in a wide range and results in large filter values. The battery is used to inject the required inertial power to the grid [20]. The battery life may decrease due to sudden load fluctuations. In [21], the author used the lithium-ion battery to provide both inertial response and primary frequency response to the grid with high penetration of wind power plants. However, using the battery at sudden peaks

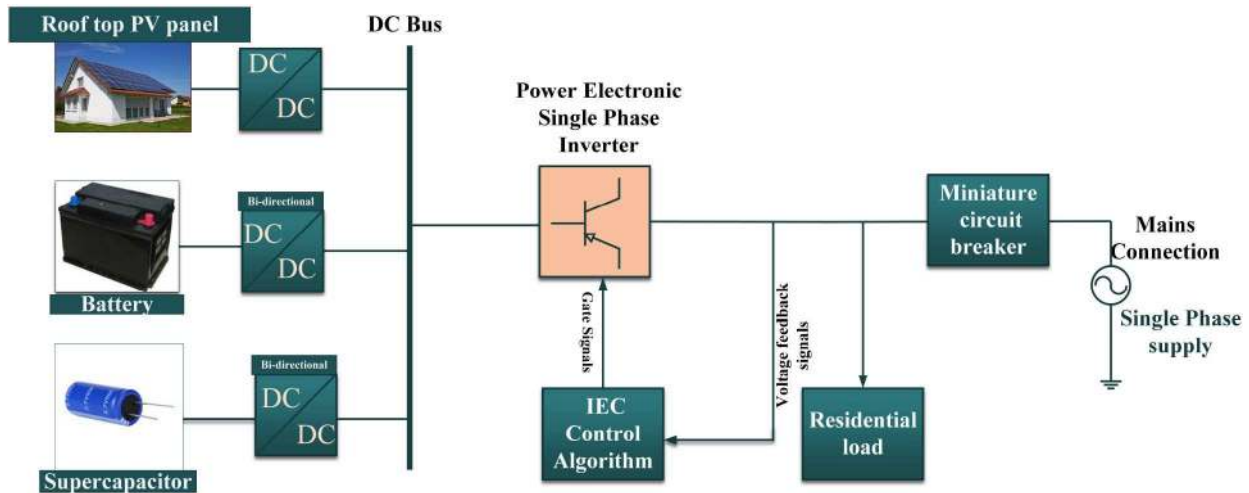


Fig. 1 Single-phase grid-connected PV inverter with HESS

increases the stress on the battery and decreases the lifetime of the battery. In [22], synchronous compensators and battery storage are used to provide the inertia and primary frequency control, respectively. However, the installation of a new synchronous condenser for inertia support is a costly option, and thus a proper analysis and study are required. In [23], the primary frequency control system uses battery storage to regulate the grid frequency under high wind power plants penetration. The battery is used in [24] to regulate the active power transfer during the microgrid's primary frequency control level.

If the large power peaks are handled by batteries, their lifespan will be reduced. On the other hand, the energy storage system like supercapacitor (SC) can able to handle the large power peaks in a short time. Hence, the combination of battery and SC is considered as an optimal solution for frequency regulation, as it provides: a lesser battery size and a longer battery life. With this hybrid energy storage system (HESS), the SC is able to provide fast power peaks and the battery can be used to slow power transients.

Several previous works have incorporated SC/battery HESS in various applications: improving overall system performance and compensated for fluctuating railway system loads in [25], extending battery life in electric buses in [26]. In [27], the combination of battery and SC is used to limit the frequency deviations in wind dominated power system. In [28], the author proved that the use of HESS instead of the battery alone has been significantly proved to decrease the money spent on primary frequency regulation by the regulation service provider. For three-phase inverter, the inertial response provided by HESS is analysed in [29, 30].

However, the frequency regulating capability for the single-phase inverter with HESS is not discussed in the literature so far as per the authors' knowledge. Hence, in this paper IEC for a single-phase grid-connected rooftop solar PV has been designed and developed to emulate the synchronous generator behaviour with battery and SC. By incorporating the IEC technique in single-phase grid-connected inverters, these single-phase inverters also can participate in the inertial response to regulate the grid frequency. A rooftop PV source along with HESS like battery and SC is connected to the grid with proper IEC algorithm can participate in the frequency regulation. The battery is used for low-frequency power variation whereas SC is used for the high-frequency power variations. HESS is used in this paper along with the PV is used to increase the efficiency, lifetime of the battery as well as to contribute the inertial service to the grid.

The objective of the paper is to incorporate frequency regulating feature to the single-phase rooftop PV-based inverters to provide the ancillary service like an inertial response to the grid under frequency variations. This paper presents the following novel features which are not discussed for the single-phase inverter context

- IEC technique for single-phase inverter is developed.

- Single-phase PV inverter is able to provide an inertial response for grid frequency deviations with IEC control and HESS.

The rest of the paper is organised as follows. Section 2 describes the system description, Section 3 discusses the core concept of IEC and control technique of HESS, Section 4 deals with the power management scheme, Section 5 discusses the real-time simulation results and discussions and Section 6 gives the conclusion.

2 System configuration

The topology of the single-phase rooftop PV inverter with HESS is shown in Fig. 1. Generally, the rooftop PV array consists of a boost converter and DC/AC inverter. The boost converter aims at extracting the maximum power from the PV system using a MPPT technique. Similarly, H-bridge inverter is used to convert the DC to AC and injects into the distribution grid. Mostly, the LCL filter is used for the rooftop PV-based inverters without transformer [31]. The HESS is connected to the DC bus via bidirectional DC-DC converters in order to maintain a constant voltage and provide an inertial response to the grid under variations in load and PV irradiance.

The system considered in this paper comprises of three power circuit stages and those are given below, the modelling of every component in the system is discussed further in this section.

- Rooftop PV array with a boost converter.
- A single-phase H-bridge inverter with LCL filter for interfacing with the grid.
- HESS with bidirectional converters.

2.1 Rooftop PV array with a boost converter

The designing of the MPPT controller for a boost converter is important for rooftop PV arrays for different irradiation levels. The boost converter used to track the maximum power from rooftop PV arrays is shown in Fig. 2. The MPPT algorithm alters the duty ratio of boost converter continuously, to track the maximum power point for different atmospheric conditions. The conventional P&O algorithm is used in this paper to track the maximum power from the rooftop PV arrays. The P&O algorithm alters the voltage slightly and measures the power; if power increases then the voltage is increased further in that direction until a change in power is zero.

2.2 Single-phase H-bridge inverter and LCL filter

A single-phase H-bridge inverter with an LCL filter is shown in Fig. 3. The LCL filter values are modelled to filter out the harmonics to maintain the total harmonic distortion in the allowable range. The ripple current and operating voltage are taken into consideration while selecting the filter values [32]. The rating

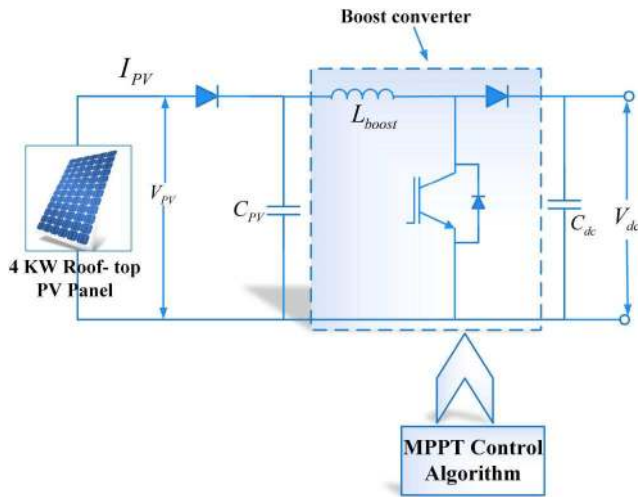


Fig. 2 Rooftop PV with a boost converter

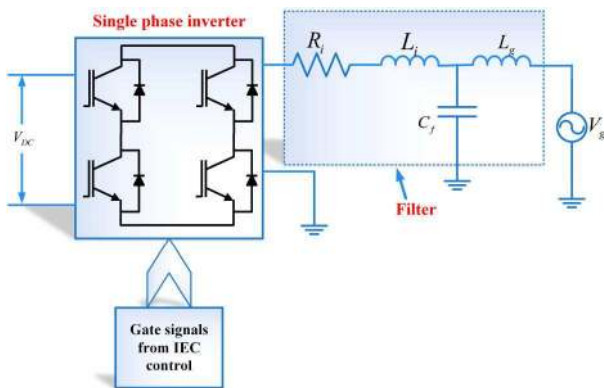


Fig. 3 Single-phase inverter with LCL filter

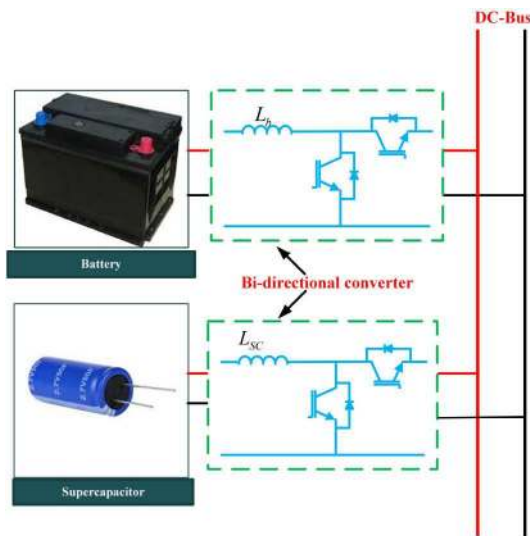


Fig. 4 HESS connected to DC-Bus

of the inverter switches is chosen by the maximum-rated power capacity.

2.3 Battery and SC system

Conventionally, the rooftop PV inverters are equipped with the battery alone. As the PV power produced is continuously fluctuating with the irradiation and temperature and operating at the maximum power point. Hence, the reserve power from PV is not available under power imbalances. So, the battery releases/absorbs the power under sudden load variations in the grid. When the power imbalance is happening suddenly and repeatedly then the

battery may experience continuous charging and discharging operations. It increases the stress on the battery and affects lifetime. To avoid this situation, extra energy storage element, the SC is connected to the grid with a bi-directional buck/boost converter. SC can react faster than a battery to offset the frequency deviation by absorbing/releasing the power in frequency deviations and PV power fluctuations. In order to add inertia as an ancillary service to the single-phase, rooftop PV inverter, HESS needs to be added with proper control. Hence, the HESS with rooftop single-phase inverter can regulate the frequency and will be able to provide the inertial response during transient conditions. The connection diagram of HESS to the DC bus is shown in Fig. 4.

To add the inertia ancillary service to the single-phase rooftop PV, the high-power density SC is needed to be added. The energy storage element like high-power density and low-energy density of SC is required to add inertial service to the power electronic inverter. The active power reserve of SC can be used as inertial power instead of rotational kinetic energy. Hence, SC is able to emulate the rotational inertia of synchronous generator to reduce the frequency deviation. The maximum storage energy of SC is mainly depending on SC voltage V_{SC} . The voltage across the SC should be maintained within the following range:

$$V_{SC,\min} < V_{SC} < V_{SC,\max} \quad (1)$$

where $V_{SC,\min}$, $V_{SC,\max}$ are the minimum and maximum operating voltages of SC. The energy stored in the SC is

$$E_{SC} = \frac{1}{2} C_{SC} V_{SC}^2 \quad (2)$$

The maximum power exchanged between the SC and grid can be known as

$$P_{SC,\max} = \pm C_{SC} V_{SC} \left| \frac{dV_{SC}}{dt} \right| \quad (3)$$

where C_{SC} is the capacitance of the SC.

3 Control schematic and design

This section deals with the design of the HESS controller along with IEC for the single-phase inverter.

3.1 Control design of HESS

The HESS is equipped with single-phase rooftop PV inverter to avoid the stress on the battery and to provide the inertial response to the grid. The controller for the HESS acts a primary role to supply the sufficient amount of power from the SC in the inertial response condition (transient condition) and power has to be release/absorb from the battery in the steady state condition. The control technique used for the HESS is shown in Fig. 5. When the frequency deviation occurs, the IEC alters the load angle for the voltage. In this time the output current of the inverter is increased and it results in a small dip in DC bus voltage. The HESS controller measures the DC bus voltage and compared with the reference voltage and in turn, gives the input to the PI controller. The PI controller generates the total current reference (I_{total_ref}) required from the HESS. This total current (I_{total_ref}) is decomposed into high-frequency reference current (I_{HFC_ref}) and the low-frequency reference current (I_{LFC_ref}). (I_{LFC_ref}) is compared to the battery current (I_{bat}) and the difference is given to the PI controller to generate the duty ratio for the battery bi-directional converter. (I_{HFC_ref}) is compared to the SC current (I_{SC}) and the difference is given to the PI controller to generate the duty ratio for the SC bi-directional converter.

3.2 Single-phase inverter control with IEC

The frequency of the grid can be regulated by using the IEC. The IEC control in single-phase inverter provides some time for the

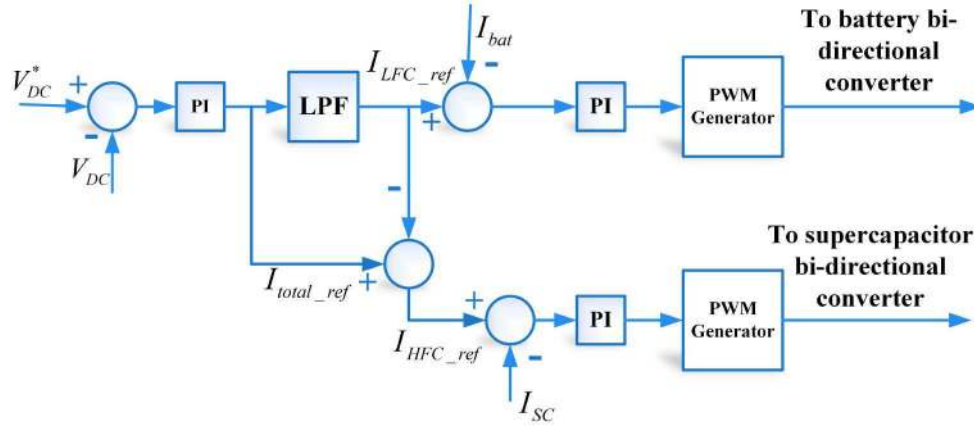


Fig. 5 HESS control technique

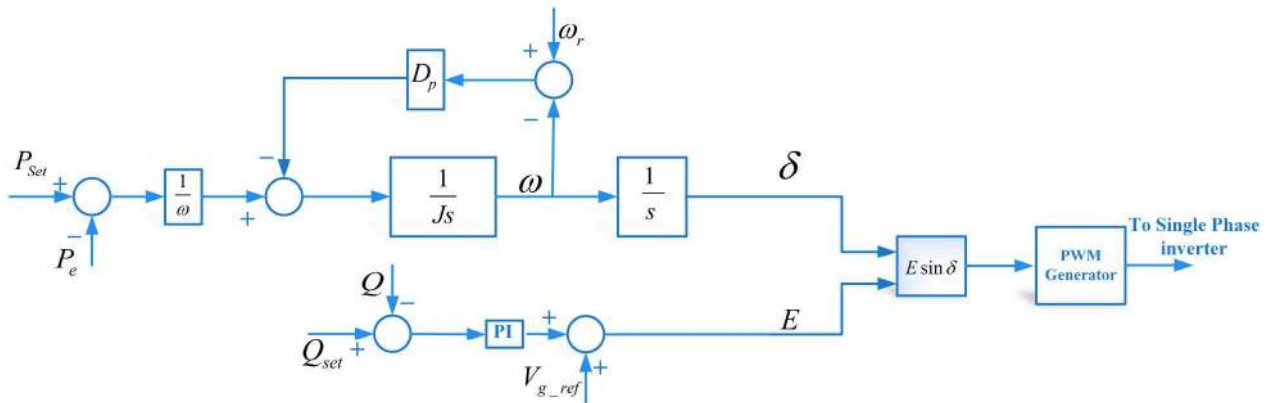


Fig. 6 IEC control for single-phase inverter

grid/primary frequency control to regulate the frequency by injecting the required amount of power using an inertial response and it is shown in Fig. 6. The main objective of this paper was to adjust the power under frequency variations on inertial response. The IEC algorithm uses the swing equation to generate the load angle δ , according to the active power change. The following equations describe the core algorithm of the IEC.

$$(P_{set} - P_e)/\omega - D_p(\omega - \omega_r) = J \frac{d\omega}{dt} \quad (4)$$

$$\frac{d\delta}{dt} = \omega \quad (5)$$

$$E = V_{g-ref} + \left(K_p + \frac{K_i}{s} \right) (Q_{set} - Q_e) \quad (6)$$

where P_{set} and Q_{set} represent the reference of active power and reactive power, respectively. P_e and Q_e are the instantaneous active power and reactive power of the system. D_p is the frequency drooping coefficient. J is the system inertia. ω and δ are the angular frequency of the system and load angle, respectively. ω_r is the reference angular frequency. E and V_{g-ref} is reference voltage amplitude generated by controller and grid voltage amplitude.

The frequency of the grid can be maintained by comparing the virtual angular frequency ω with the angular frequency reference ω_r and multiplied with the gain D_p , to get the damping torque. The difference of P_{set} and P_e is divided by reference angular frequency and the result is added with damping torque. The resultant signal is applied to an integrator with the gain to get the angular speed of the inverter. Likewise, the regulation of the voltage amplitude of the grid can be done. The difference between the reactive power measured and set value is calculated and this difference is given to the PI controller. The PI controller generates the required voltage amplitude for the error and it is added to the reference voltage value. Whenever there is a change in the grid frequency, the IEC

supports the inertial response by injecting/absorbing the power for a few seconds with the help of SC and battery.

Implementation of IEC in single-phase inverter reduces the frequency deviations and the high rate of change of frequency (ROCOF) of the grid. The inertia constant of the IEC is chosen such that the stability of the IEC-based inverter in the allowable limit. If the inertia constant is increases then the IEC becomes slow.

4 Power management scheme

To accomplish the inertia support from rooftop PV and HESS with IEC control, a power management strategy is required. Fig. 7 illustrates the power management scheme for rooftop PV and HESS with inertia control. Since frequency regulation mostly depends upon the active power imbalance. So, the control blocks relating to reactive power in Fig. 6 are not considered here. Measure the angular frequency (ω) of the system and calculate frequency deviation $\Delta\omega$

$$\Delta\omega = \omega_r - \omega \quad (7)$$

As being demonstrated in Fig. 8, the power fluctuations under sudden disturbance occurs either from the load or from PV source can be decomposed into high frequency, medium frequency and low frequency power components [33]. Irrespective of the grid condition (ON/OFF), the SC responds first to deliver the power for frequency component which is greater than f_H . The battery is used to support the middle frequency component of power ($f_H > f > f_L$). Thereby delivering the inertial response from HESS to the grid. The remaining low-frequency component power ($f < f_L$) is delivered by the grid to balance the power imbalance when the grid is available otherwise, the battery would deliver the power to the load.

When the supply from the grid/mains is in ON condition, the power imbalance is allocated on the basis of

$$\Delta P = P_{SC} + P_{Bat} + P_{Grid} \quad (8)$$

$$E_{KE} = \frac{1}{2} J \omega_s^2 \quad (10)$$

When the supply from the grid is in OFF condition, the power imbalance is allocated on the basis of

$$\Delta P = P_{SC} + P_{Bat} \quad (9)$$

The energy stored in the rotor of the synchronous generator is used to arrest the frequency deviation and it is replaced by the energy stored in the SC in this paper to arrest the frequency deviation. The energy stored in the rotor is known as

where J is the inertia and ω_s is the synchronous speed of the machine. By equating (2) and (9) the value of the SC can be derived as

$$C_{SC} = \frac{J \omega_0}{V_0 \Delta V_{SC}} \Delta \omega \quad (11)$$

where, ω_0 is the nominal angular frequency, V_0 is the nominal DC bus voltage. Hence, the selection of capacitance of the SC mainly

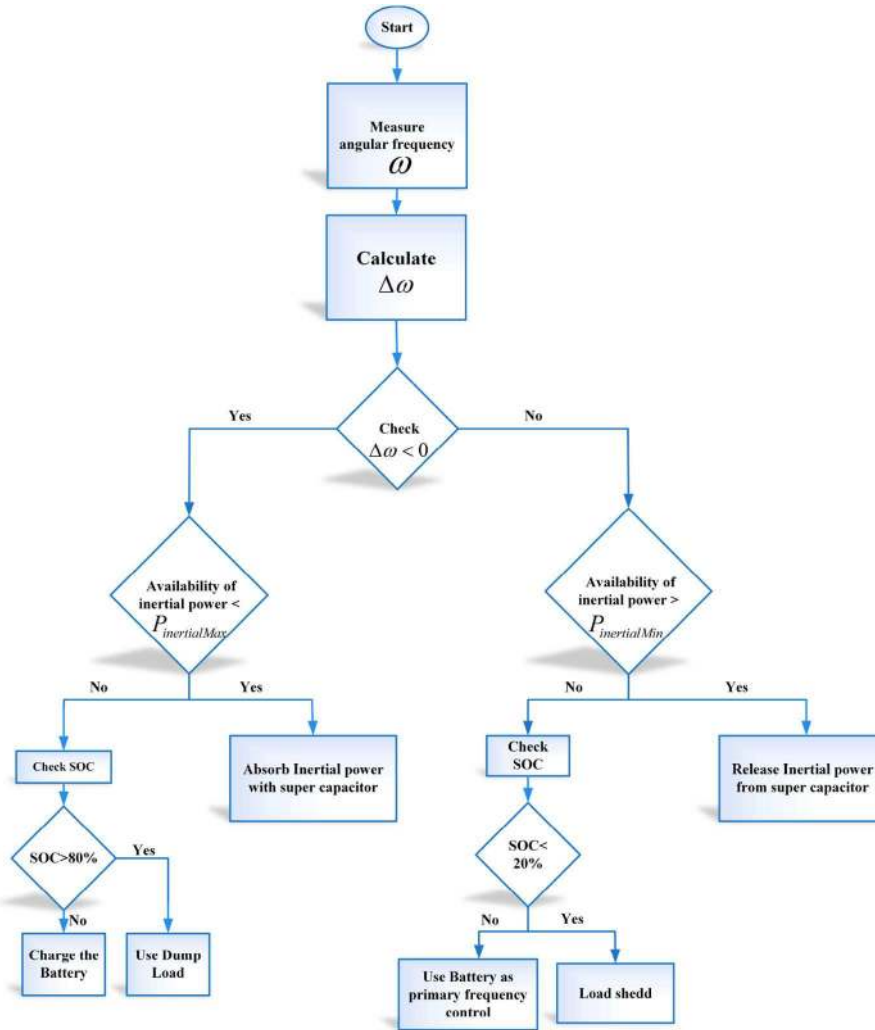


Fig. 7 Working flow chart of IEC control with HESS for rooftop solar PV

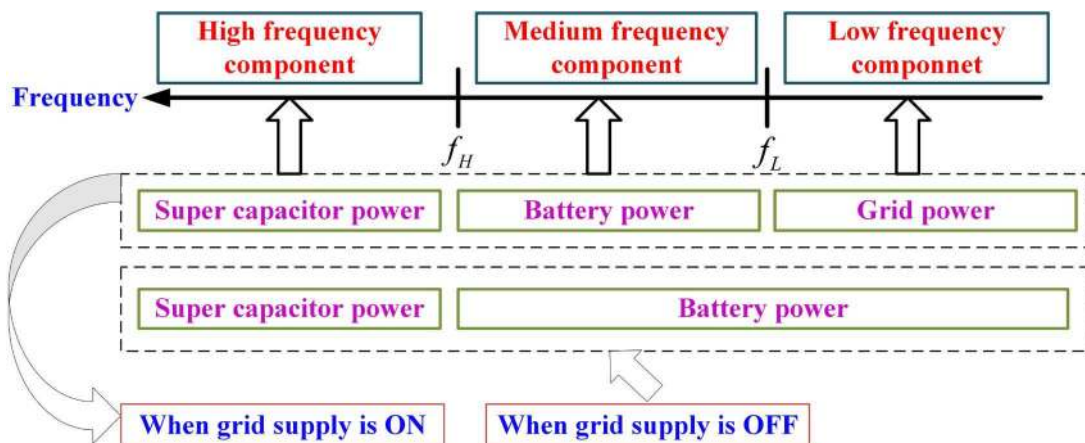


Fig. 8 Illustration of power smoothing principle under disturbances

Table 1 System and control parameter values

Parameters	Specification
PV power	4kW
DC-bus voltage	400V
DC-bus capacitor	1650 μ F
grid voltage	230V
nominal grid frequency (f)	50Hz
inverter side filter inductance (L_i)	2.4mH
grid side filter inductance (L_g)	0.4 mH
filter capacitance (C)	12 μ F
drooping coefficient (D_p)	2.2
total inertia constant (H)	1.3
SC inertia constant (H_{SC})	0.24

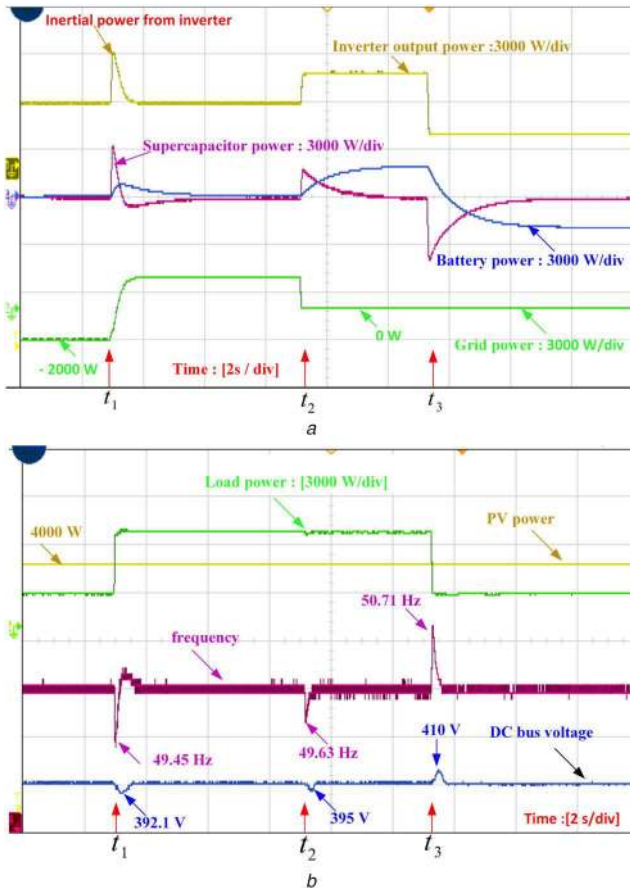


Fig. 9 Real power variations at constant irradiation variable load
(a) Inverter output power, SC power, battery power, grid power, (b) Load demand, PV power, frequency and DC bus voltage

depends on allowed frequency deviation and allowed DC bus voltage deviation.

Fig. 7 depicts the working flow chart of single-phase PV inverter with HESS control, where $P_{inertialMax}$ is the above which the SC cannot absorb the power and $P_{inertialMin}$ is the below which the SC cannot supply the power. The operation of IEC mainly depends on measuring of angular frequency and it is divided into two scenarios: (i) the angular frequency is more than the reference value and (ii) The angular frequency is less than the nominal value.

Case i: If the angular frequency is more than the nominal value, then the load demand is less than the generated power. If the power at the SC is less than $P_{inertialMax}$, then the extra power is absorbed with SC using IEC control. Else control algorithm at the battery would act as the primary frequency controller to bring back the frequency to the nominal value. If SOC is $<80\%$, then charge the battery or else use the dump load to utilise the excess power in the system.

Case ii: If the frequency is less than the nominal value, then the generated power is less than the load demand. If the power at the SC greater than $P_{inertialMin}$, then release the required power with SC using IEC. Else control algorithm at the battery would act as the primary frequency controller to bring back the frequency to the nominal value. If SOC is $>20\%$ then supply the load from the battery and reduces the frequency deviation else the load shedding takes place.

5 Real-time simulation results and discussions

The concept of single-phase IEC discussed in the earlier section has been validated with the real-time simulations. The entire system is shown in Fig. 1 along with the controllers loaded into OP5700 real-time simulator to test the performance, and four channel mixed-signal oscilloscope (Keysight InfiniiVision 3000) is used to capture the waveforms from the real-time simulator. The parameters of the IEC controller and inverter used in the real-time simulations are listed out in Table 1.

In this paper, 4 kW of PV source is considered with 200 V and 20 A of voltage and current ratings, respectively. The boost converter was designed according to the current-carrying capacity. The grid was assumed to have a short circuit capacity of 20 KVA. Real-time simulation tests are conducted to demonstrate the performance of the single-phase rooftop PV inverter and HESS with IEC control in frequency support.

Case 1: load changes at constant irradiance. In this case, the performance of single-phase IEC under step increase in load demand under constant irradiance is analysed. In a synchronous generator, whenever the step increase in load occurs, then the kinetic energy stored in the rotor is released or absorbed. This helps to decrease of ROCOF and frequency deviation is known as an inertial response. In the same way, the IEC has to release the power when the frequency dip occurs. The rooftop PV is operating at the MPPT technique. At the 1000 W/m^2 irradiance, the maximum power 4000 W is extracted from the rooftop PV. In the initial stage, the local load is considered as 2000 W and the remaining power generated from the PV is injected to the grid. The real power variations of the inverter, SC, battery and grid are shown in Fig. 9a. The variation in frequency, DC bus voltage, Load demand and PV power is shown in Fig. 9b. At $t = t_1$ s, another 4000 W load is activated, then the frequency starts to fall and it is shown in Fig. 9b. The IEC algorithm activates when the frequency of the grid deviates from the reference frequency. The IEC injects the inertial power when there is a frequency deviation to support the grid frequency. The inertial response from the inverter is delivered the active power before the grid supplying the power is shown in Fig. 9a. Whenever there is a dip in the frequency SC releases the power to arrest the frequency deviation before the battery and grid in the inertial response. In this scenario, it is clearly observed from Fig. 9a that, the high-frequency power component is delivered by SC, medium frequency power component is supplied from the battery, followed by the low-frequency power component supplied from the grid and proved (8).

At $t = t_2$ s supply from the mains is lost, then the frequency starts to deviate due to the power imbalance. So, the IEC activates and initiates the power supply from HESS to decrease the frequency imbalance. In this scenario, the high-frequency power component is supplied from SC, medium and low-frequency power component is supplied from the battery and proved (9).

At $t = t_3$ s one of the loads is switched off suddenly, hence, the frequency starts to rise due to the power imbalance. In this situation, IEC decreases the load angle to decrease the power flow and excess energy generated from the PV is used to charge the battery. Depending on power imbalance, the high-frequency power component is absorbed from the SC and low-frequency power component is absorbed from the battery.

Case 2: Irradiance change at constant load. In this case, the performance of single-phase IEC during PV irradiation changes under constant load is analysed. The single-phase PV-HESS with

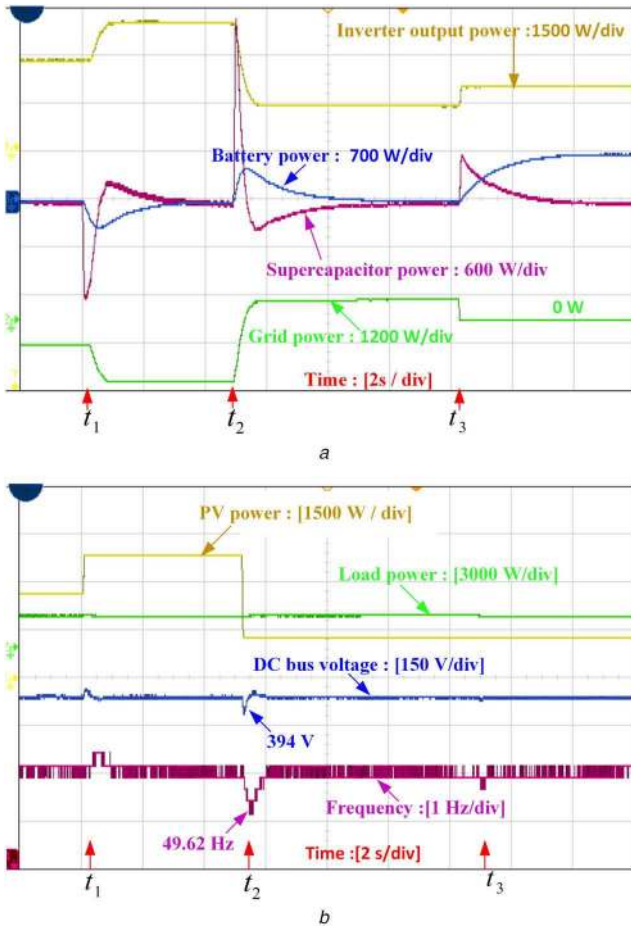


Fig. 10 Real power variations at variable irradiation and constant load (a) Inverter output power, SC power, battery power, grid power, (b) Load demand, PV power, frequency and DC bus voltage

IEC control should be able to supply the real power, under variable irradiation levels. Initially, the PV is operating at 700 W/m^2 and maximum power output generated is 2800 W and the constant load considered in this case is 2000 W and the remaining 800 W is injected into the grid. Later, a step change in solar irradiation at the rate of 1000 W/m^2 and 500 W/m^2 were modelled at $t = t_1 \text{ s}$ and $t_2 \text{ s}$, respectively. The real power variations of the inverter, SC, battery and grid are shown in Fig. 10a. The variation in frequency, DC bus voltage, load demand and PV power is shown in Fig. 10b.

At $t = t_1 \text{ s}$, the irradiation is increased then step increase in the PV output power is observed from Fig. 10b and the excess amount generated from the PV source is fed to the grid (total power injected to the grid from PV is increased) shown in Fig. 10a. In this transition, the small rise in frequency and DC bus voltage is observed. The high-frequency power component is absorbed by SC, the medium frequency component is absorbed from the battery and low-frequency component of power is injected into the grid.

At $t = t_2 \text{ s}$ the solar irradiation is decreased from 1000 to 500 and MPPT algorithm tried to extract the maximum power of 1450 W from the PV panel. The power generated from the PV is not sufficient to meet the load demand. Hence, the remaining required power drawn from the grid. This power imbalance situation creates the small dip in frequency and DC bus voltage. The high-frequency power component is released from SC, medium frequency power component is supplied from battery and low-frequency power component is supplied from grid.

At $t = t_3 \text{ s}$ the power supply from the mains is lost, then the power imbalance is supplied from the battery. In this scenario, the SC releases the high-frequency power component to arrest the frequency deviation and battery supplies the medium and low-frequency power component to bring back the frequency to the nominal value and to balance the power.

In all the power imbalance scenarios, the SC would act first to counteract the power imbalance and to arrest the frequency deviation in the inertial response and later, battery/grid would act to bring back the frequency to the nominal value.

6 Conclusion

This paper has implemented an IEC control for single-phase rooftop PV-HESS system to provide the ancillary service (inertial service) to the grid under frequency variations. The SC is used to emulate the inertia of the synchronous generator to arrest the frequency deviation and battery is used to bring back the frequency to the nominal value. The proposed single-phase PV-HESS combination along with IEC control effectively control the frequency under load side variations. Furthermore, it has been shown that the control technique regulates the frequency under PV irradiation variations also. The real-time simulation results prove that a grid-connected single-phase PV-HESS inverter with IEC control technique able to provide the inertial support to the grid to improve the stability.

7 Acknowledgment

Authors like to acknowledge the funding agencies for the supported received for this project activities by Grant Project No. SR/FST/ETI-420/2016(C) "Fund for Improvement of S&T infrastructure in Universities & Higher Educational Institutions (FIST)" Department of Science and Technology (DST)-Government of India. Funded to establish the PHIL set-up which is a part of this research project. Also, this research activity is supported by Danida Fellowship Mobility Grant Project No. "19-MG05-AAU", Government of Denmark for "Renewable Energy Penetration in Microgrids and Electric Vehicles Charging Station".

8 References

- [1] Solangi, K.H., Islam, M.R., Saidur, R., *et al.*: 'A review on global solar energy policy', *Renew. Sust. Energy Rev.*, 2011, **15**, (4), pp. 2149–2163
- [2] Fu, X., Member, S., Li, S., *et al.*: 'Control of single-phase grid-connected converters with LCL filters using recurrent neural network and conventional control methods', *IEEE Trans. Power Electron.*, 2016, **31**, (7), pp. 5354–5364
- [3] Abhijit Kulkarni, V.J.: 'Mitigation of lower order harmonics in a grid-connected single-phase PV inverter', *IEEE Trans. Power Electron.*, 2013, **28**, (11), pp. 5024–5037
- [4] Dasgupta, S., Member, S., Sahoo, S.K.: 'Single-phase inverter-control techniques for interfacing renewable energy sources with microgrid — part II: series-connected inverter topology to mitigate voltage-related problems along with active power flow control', *IEEE Trans. Power Electron.*, 2011, **26**, (3), pp. 732–746
- [5] Yang, Y., Zhou, K., Member, S., *et al.*: 'Current harmonics from single-phase grid-connected inverters — examination and suppression', *IEEE J. Emerging Sel. Topics Power Electron.*, 2016, **4**, (1), pp. 221–233
- [6] Inverter, S.-P., Li, X., Member, S., *et al.*: 'Direct instantaneous ripple power predictive control for active ripple decoupling of single-phase inverter', *IEEE Trans. Ind. Electron.*, 2018, **65**, (4), pp. 3165–3175
- [7] Schonardie, M.F., Ruseler, A., Coelho, R.F., *et al.*: 'Three-phase grid-connected PV system with active and reactive power control using dq0 transformation'. INDUSCON.2010.574000, May 2014
- [8] Suyata, T.-I., Po-ngam, S.: 'Simplified active power and reactive power control with MPPT for three-phase grid-connected photovoltaic inverters'. 2014 11th Int. Conf. on Electrical Engineering/Electronics, Computer, Telecommunications and Information Technology (ECTI-CON), Nakhon Ratchasima, Thailand, 2014, pp. 1–4
- [9] Ninad, N.A., Rufer, A.: 'A vector controlled single-phase voltage source inverter with enhanced dynamic response'. 2010 IEEE Int. Symp. on Industrial Electronics, Bari, Italy, 2010, pp. 2891–2896
- [10] Samerchur, S., Premrudeepreechacharn, S., Kumsuwun, Y., *et al.*: 'Power control of single-phase voltage source inverter for grid-connected photovoltaic systems'. 2011 IEEE/PES Power Systems Conf. and Exposition, Phoenix, Arizona, USA, 2011, pp. 1–6
- [11] Monfared, M., Sanatkar, M., Golestan, S.: 'Direct active and reactive power control of single-phase grid-tie converters', *IET Power Electron.*, 2012, **5**, (8), pp. 1544–1550
- [12] Zhong, Q.-C.C., Weiss, G., Member, S., *et al.*: 'Synchronverters: inverters that mimic synchronous generators', *IEEE Trans. Ind. Electron.*, 2011, **58**, (4), pp. 1259–1267
- [13] Alipoor, J., Miura, Y., Ise, T.: 'Power system stabilization using virtual synchronous generator with alternating moment of inertia', *IEEE J. Emerging Sel. Topics Power Electron.*, 2015, **3**, (2), pp. 451–458
- [14] Paper, C., Visscher, K., Grid, F., *et al.*: 'Virtual synchronous generators'. Proc. IEEE PES Meeting, Pittsburgh, PA, August 2008, 2014

- [15] Zhang, W., Remon, D., Rodriguez, P.: 'Frequency support characteristics of gridinteractive power converters based on the synchronous power controller', *IET Renew. Power Gener.*, 2017, **11**, (4), pp. 470–479
- [16] Suul, J.A., D'Arco, S., Guidi, G.: 'Virtual synchronous machine-based control of a single-phase bi-directional battery charger for providing vehicle-to-grid services', *IEEE Trans. Ind. Appl.*, 2016, **52**, (4), pp. 3234–3244
- [17] Zeng, Z., Zhao, R., Yang, H., *et al.*: 'Single-phase virtual synchronous generator for distributed energy sources'. 2013 Int. Conf. on Electrical Machines and Systems (ICEMS), Busan, South Korea, 2013, pp. 190–195
- [18] Younis, T., Ismeil, M., Hussain, E.K., *et al.*: 'Improved single-phase self-synchronised synchronverter with enhanced dynamics and current limitation capability', *IET Power Electron.*, 2019, **12**, pp. 337–344
- [19] Li, H., Zhang, X., Shao, T., *et al.*: 'Flexible inertia optimization for single-phase voltage source inverter based on hold filter', *IEEE J. Emerging Sel. Topics Power Electron.*, 2019, **7**, (2), pp. 1300–1310
- [20] Mishra, S., Pullaguram, D., Buragappu, S.A., *et al.*: 'Single-phase synchronverter for a grid-connected roof-top photovoltaic system', *IET Renew. Power Gener.*, 2016, **10**, (8), pp. 1187–1194
- [21] Knap, V., Sinha, R., Swierczynski, M., *et al.*: 'Grid inertial response with lithium-ion battery energy storage systems'. IEEE Int. Symp. on Industrial Electronics, Istanbul, Turkey, 2014, pp. 1817–1822
- [22] Mosca, C., Arrigo, F., Mazza, A., *et al.*: 'Mitigation of frequency stability issues in low inertia power systems using synchronous compensators and battery energy storage systems', *IET Gener. Transm. Distrib.*, 2019, **13**, (17), pp. 3951–3959
- [23] Tan, J., Zhang, Y.: 'Coordinated control strategy of a battery energy storage system to support a wind power plant providing multi-timescale frequency ancillary services', *IEEE Trans. Sustain. Energy*, 2017, **8**, (3), pp. 1140–1153
- [24] Serban, I., Marinescu, C.: 'Control strategy of three-phase battery energy storage systems for frequency support in microgrids and with uninterrupted supply of local loads', *IEEE Trans. Power Electron.*, 2014, **29**, (9), pp. 5010–5020
- [25] Ise, T., Kita, M., Taguchi, A.: 'A hybrid energy storage with a SMES and secondary battery', *IEEE Trans. Appl. Supercond.*, 2005, **15**, (2) PART II, pp. 1915–1918
- [26] Li, J., Zhang, M., Yang, Q., *et al.*: 'SMES/battery hybrid energy storage system for electric buses', *IEEE Trans. Appl. Supercond.*, 2016, **26**, (4), pp. 1–5
- [27] Cao, J., Du, W., Wang, H., *et al.*: 'Optimal sizing and control strategies for hybrid storage system as limited by grid frequency deviations', *IEEE Trans. Power Syst.*, 2018, **33**, (5), pp. 5486–5495
- [28] Akram, U., Khalid, M.: 'A coordinated frequency regulation framework based on hybrid battery-ultracapacitor energy storage technologies', *IEEE. Access.*, 2017, **6**, pp. 7310–7320
- [29] Fang, J., Tang, Y., Li, H., *et al.*: 'A battery/ultracapacitor hybrid energy storage system for implementing the power management of virtual synchronous generators', *IEEE Trans. Power Electron.*, 2018, **33**, (4), pp. 2820–2824
- [30] Rocabert, J., Capo-Misut, R., Munoz-Aguilar, R.S., *et al.*: 'Control of energy storage system integrating electrochemical batteries and supercapacitors for grid-connected applications', *IEEE Trans. Ind. Appl.*, 2019, **55**, (2), pp. 1853–1862
- [31] González, R., López, J., Sanchis, P., *et al.*: 'Transformerless inverter for single-phase photovoltaic systems', *IEEE Trans. Power Electron.*, 2007, **22**, (2), pp. 693–697
- [32] Ahmed, K.H., Finney, S.J., Williams, B.W.: 'Passive filter design for three-phase inverter interfacing in distributed generation', *Compat. Power Electron.*, 2007, **22**, pp. 693–697
- [33] Xiao, J., Bai, L., Li, F., *et al.*: 'Sizing of energy storage and diesel generators in an isolated microgrid using discrete Fourier transform (DFT)', *IEEE Trans. Sustain. Energy*, 2014, **5**, (3), pp. 907–916